International Immunology, Vol. 15, No. 2, pp. 187–195
doi: 10.1093/intimm/dxg018, available online at www.intimm.oupjournals.org

Evidence to support the cellular mechanism involved in serum IgG homeostasis in humans

E. Sally Ward[1,2], Jinchun Zhou[1], Victor Ghetie[2] and **Raimund J. Ober[2]**

[1]Center for Immunology and [2]Cancer Immunobiology Center, University of Texas Southwestern Medical Center, 6000 Harry Hines Boulevard, Dallas, TX 75390-8576, USA

Keywords: FcRn, human IgG1, immunodeficiency, lysosomal trafficking, serum persistence

Abstract

IgG is the most abundant serum antibody and is an essential component of the humoral immune response. It is known that the 'neonatal' Fc receptor (FcRn) plays a role in maintaining constant serum IgG levels by acting as a protective receptor which binds and salvages IgG from degradation. However, the cellular mechanism that is involved in serum IgG homeostasis is poorly understood. In the current study we address this issue by analyzing the intracellular fate in human endothelial cells of IgG molecules which bind with different affinities to FcRn. The studies show that IgG which do not bind to FcRn accumulate in the lysosomal pathway, providing a cellular explanation for short serum persistence of such antibodies. We have also investigated the saturability of the homeostatic system and find that it has limited capacity. Our observations have direct relevance to the understanding and treatment of IgG deficiency, and to the effective application of therapeutic antibodies.

Introduction

IgG represents the most abundant serum Ig and plays an essential role in mediating immunity. Knowledge as to how serum IgG levels are maintained at constant levels in the circulation is of central importance in understanding the regulation of humoral immunity. For example, such information has obvious relevance to the analysis and treatment of human IgG (hIgG) deficiencies, in addition to the effective delivery of antibodies for passive immunization and targeted immunotherapy. Despite this, there is limited knowledge of the cellular and molecular processes which regulate serum IgG levels. In a classic paper (1), Brambell *et al*. put forward a hypothesis to explain serum IgG homeostasis. This hypothesis proposed that salvage receptors in cells of unknown type acted to bind and recycle pinocytosed IgG molecules back into the serum. Brambell *et al*. also suggested that these receptors were involved in the transmission of maternal IgG from mother to young. The putative receptors were believed to be saturable, so that any IgG molecules not receptor bound following pinocytosis would suffer degradation. This hypothesis was put forward in the absence of any knowledge of the receptor or cell types involved, but at the conceptual level provided a satisfactory model by which IgG homeostasis could be maintained.

More recent studies in mice indicate that the 'neonatal' Fc receptor (FcRn; n = neonatal) is the salvage receptor which regulates IgG levels (2–4). These studies were carried out in mice that do not express functional FcRn and showed that lack of this Fc receptor results in hypercatabolism of IgG. Expression of this Fc receptor is not only restricted to the pre- or neonatal period when it plays a role in the delivery of maternal IgG to offspring (5–8), but can also be ubiquitously found in endothelial cells of adult tissues where it is believed to be involved in IgG homeostasis (2,9). Thus, at the level of identification of the receptor, the details of the Brambell hypothesis (1) have been clarified. In contrast, although subsequent models which are based on the Brambell hypothesis have been elaborated (10,11), there is still limited knowledge concerning the events that occur at the cellular level to regulate serum IgG homeostasis. Here we address this issue by comparing the intracellular trafficking of wild-type IgG1 and a site-specifically mutated variant that does not bind to FcRn. Any differences in trafficking between these anti-

Correspondence to: E. S. Ward; E-mail: sally.ward@UTSouthwestern.edu

Transmitting editor: D. Fearon

Received 31 July 2002, *accepted* 30 October 2002

bodies can therefore be unequivocally attributed to loss of interaction with this Fc receptor. Significantly, our studies have been carried out in microvasculature-derived human endothelial cells and are therefore of direct physiological relevance to understanding IgG homeostasis.

Primarily due to the obvious ethical constraints of carrying out experiments in humans, much less is known about human FcRn than rodent FcRn. A human homolog of rodent FcRn has been isolated from human syncytiotrophoblasts (12). The use of an *ex vivo* placental model has implicated FcRn in the delivery of IgG across the maternofetal barrier (13), indicating that as in rodents, human FcRn is an IgG transporter. There is generally a good correlation between binding affinity of an IgG for FcRn and serum half-life in both mice and humans (14–16). Human and rodent FcRn therefore appear to serve similar functions. However, it has recently been shown that human and mouse FcRn have significant differences in binding specificity (16), with human FcRn being highly selective in binding specificity for IgG from a limited number of species. In contrast, mouse FcRn does not show this stringency and binds to IgG of every species analyzed (16). As a consequence of this marked difference in binding specificity, caution should be exercised in extrapolating data from functional assays for FcRn in mice to humans.

The amino acids involved in the FcRn–IgG interaction have been mapped using both functional and structural studies (14,17–22). IgG residues that are involved in binding to FcRn are located at the C_H2–C_H3 domain interface of the Fc region. Using this knowledge, the molecular basis for the effects of mutations of IgG or Fc fragments on FcRn binding affinity can generally be rationalized. However, knowledge of the intracellular fate of IgG which bind with different affinities to FcRn is very limited. In addition, there is a paucity of data concerning the intracellular trafficking of IgG in cells where FcRn is expressed endogenously, such as in endothelial cells (9). There is also no information concerning the concentration dependence of IgG uptake and how this might affect recycling versus degradation, i.e. the capacity of the homeostatic system.

In the current study we compare the trafficking of wild-type hIgG1 and IgG which do not bind to FcRn in human endothelial cells. These latter IgG include a variant of hIgG1 in which mutation of His435 to alanine results in selective loss of binding to FcRn with retention of all other Fc-mediated functions (13). The effects of IgG concentration on IgG trafficking have also been investigated. Our analyses provide direct evidence to support the concept that the function of human FcRn expression in endothelial cells is to regulate serum IgG levels, where it behaves as a saturable receptor of limited capacity.

Methods

Cell lines

HULEC-5A cells (SV-40 large T antigen-transformed line derived from human lung microvasculature; F. Candal, pers. commun.) were obtained from the Center for Disease Control, and maintained in phenol red-free Ham12K medium (Biosource, Camarillo, CA) containing 30 μg/ml endothelial cell growth supplement, 100 μg/ml heparin, 2 mM glutamine, 135 μg/ml $CaCl_2$ and 10% FCS. FCS was passed through Protein G–Sepharose to deplete IgG prior to adding to medium. Cells were not used in experiments beyond 23 passages as they reach senescence around passage 25 (F. Candal, pers. commun.).

RT-PCR

RNA was isolated from HULEC-5A cells using the RNAzol method (Tel-Test, Friendswood, TX). cDNA was synthesized using standard methods of molecular biology and oligonucleotide primers specific for human FcRn (matching or complementary to bases 576–600 or 1072–1098). Aliquots of cDNA were used in the PCR with several primer pairs specific for FcRn (bases 74–97 and 576–600; 799–819 and 1072–1098; and 584–609 and 1072–1098 of human FcRn). As a positive control, primers specific for the 5′ (leader peptide) and 3′ ends of the human β_2-microglobulin gene (size 357 bp) were used. PCR products were analyzed by agarose gel electrophoresis.

Immunofluorescence staining

HULEC-5A cells were grown on coverslips and fixed with 3.4% paraformaldehyde, permeabilized with 0.1% Triton and incubated with PBS/1% BSA for 15 min at room temperature. For anti-EEA-1 staining, cells were incubated with 5 μg/ml anti-EEA-1 (BD Transduction, San Diego, CA) or control irrelevant mouse IgG1 (mIgG1) for 45 min, washed and incubated in 2 μg/ml Alexa 488-labeled anti-mIgG (extensively cross-adsorbed; Molecular Probes, Eugene, OR) for 45 min. Cells were washed and coverslips mounted using Prolong (Molecular Probes).

Antibodies and labeling with Alexa fluor

Wild-type hIgG1 [HuLys10; κ (23)] and a mutated derivative (His435 to Ala; H435A) that does not bind to FcRn (13) were used in these studies. These humanized IgG are specific for hen egg lysozyme (HEL) and were purified from culture supernatants using HEL–Sepharose (23). The cell line expressing HuLys10 (23) was a generous gift of Dr Jeff Foote (Fred Hutchinson Cancer Center, Seattle, WA). hIgG1 (κ) was purchased from Sigma (St Louis, MO). RFB4 or HD37 [anti-CD22 and anti-CD19 respectively (24)] were used as sources of mIgG1. IgG were labeled with Alexa Fluor 647 ('Alexa 647') using Alexa Fluor 647 succinimidyl ester (Molecular Probes) and the protocol recommended by the manufacturer. Following extensive dialysis or the use of a Sephadex G-25 column to remove free fluorophore, Alexa 647 incorporation into IgG was assessed by A_{650nm} values. For all comparative studies, IgG with similar levels of fluorophore incorporation were used. Unlabeled hIgG (a mixture of all four hIgG isotypes; designated IVIg) were purified using Protein G–Sepharose from commercially available Sandoglobulin (a mixture of pooled hIgG with minor amounts of IgA for use in therapy; generously provided by Dr Richard Wasserman). Protein concentrations were determined using BCA protein assay kits (Pierce, Rockford, IL) and/or OD_{280nm} values.

Surface plasmon resonance (SPR)

SPR was used to assess the activity of the Alexa 647-labeled IgG following addition to the labeling mixes that were added to HULEC-5A cells (see below). CM5 sensor chips were coupled with recombinant mouse FcRn (25) at a density of 1724 RU. Mouse FcRn was used in preference to human FcRn for these experiments as we have found that it is more stable on the sensor chip surface. Mouse FcRn binds to hIgG1 and mIgG1, but not to H435A (13). In addition, for use as a reference cell, one flow cell was treated with coupling buffer only during the coupling reaction. Labeling mixes (in medium, pH 7) were diluted 10-fold in PBS (pH 6.0) plus 0.01% Tween 20 (so that the pH was permissive for binding) and injected at a flow rate of 10 μl/min. Bound IgG was 'stripped' from the chip during the dissociation phase by injection of PBS (pH 7.2) plus 0.01% Tween 20. Data were processed by zero adjusting and reference cell subtraction using BIAevaluation 3.0 software.

Analysis of IgG trafficking by pulse chase experiments

HULEC-5A cells were grown on coverslips in 24-well plates and pulsed with mixtures of Alexa 647-labeled IgG (at concentrations indicated in legends) and 5 μg/ml DiI-labeled low-density lipoprotein (DiI-LDL; Molecular Probes) for 20 min at 37°C in a 5% CO_2 incubator. In some experiments, DiI-LDL was replaced with 0.5 mg/ml Alexa 546-labeled dextran (M_r 10,000, lysine fixable; Molecular Probes). All mixtures were prewarmed to 37°C prior to addition to cells. In some experiments, Alexa Fluor 488 ('Alexa 488')-labeled holotransferrin (Tf; Molecular Probes) was added to the mixtures at 100 μg/ml. Immediately following the pulse period, cells were washed 3 times with ice-cold PBS (pH 7.2) and either fixed immediately or incubated in prewarmed (37°C) chase medium. Chase medium contained unlabeled IVIg at the concentration of labeled IgG used to pulse the cells and, if Alexa 488 Tf was used, unlabeled Tf (Sigma) at 2 mg/ml. Cells were chased at 37°C in a CO_2 incubator for 10, 20 or 40 min (as indicated), washed 3 times with cold PBS and fixed. Cells were fixed by treatment with 3.4% paraformaldehyde at room temperature for 30 min, then washed 3 times with cold PBS and mounted in Prolong (Molecular Probes). In all experiments, cell samples for background autofluorescence were prepared by using the same treatment without the fluorescent labels. Also, to analyze 'bleed through' from one fluorophore to another during imaging with the different filter sets (see below), cells were also labeled individually with each fluorophore.

Flow cytometry

HULEC-5A cells were pulse-chased with different concentrations of Alexa 647-labeled mIgG1 or wild-type hIgG1 (HuLys10) using the same protocol as above. Cells were removed by treatment with 5 mM EDTA/PBS or trypsin, washed and analyzed by flow cytometry using a FACSCalibur. Data was processed and geometric mean intensities determined using WinMDI 2.8 (http://facs.scripps.edu). For geometric mean intensity values, background autofluorescence values of cells treated with medium only were subtracted.

Fluorescence microscopy

Images were acquired using a Zeiss Axiovert 100TV inverted fluorescence microscope with a ×100 PlanApo objective. For Alexa 488, a Zeiss/Chroma filter set was used (Ex: D470/40; Em: D535/40; Bs: 500DCLP). DiI-LDL and Alexa 647-labeled IgG were imaged using a Chroma HQ:TRITC/DII filter set (Ex: HQ545/30; Em: HQ610/75; Bs: Q570LP) and a Chroma HQ:cy5 filter set (Ex: HQ620/60; Em: HQ700/75; Bs: Q660LP) respectively. Images were acquired with a cooled 12-bit Hamamatsu (Shizuoka, Japan; Orca100) camera using custom-written software. For Alexa 647-labeled IgG, images acquired with the same exposure times and lamp power were compared. In all cases, background fluorescence levels (obtained from cells treated with medium only during labeling; see above) at the exposure times used for each fluorophore were analyzed and found to be negligible. In addition, 'bleed through' of one fluorophore into the filter set of a distinct fluorophore was at background levels.

Data processing

Images were overlaid in the software package Matlab, exported in TIFF format and incorporated for presentation in Canvas 8. No processing was performed on the images. For visualization purposes, Alexa 647 is represented in the images as green (Figs 3–5) or red (Fig. 6).

Results

A human endothelial cell line derived from microvasculature (HULEC-5A) was used in these studies. Microvasculature-derived cells were used in preference to endothelial cells isolated from large vessels as analyses in mice indicate that FcRn is preferentially expressed in microvessels (9). Expression of human FcRn in HULEC-5A cells could be detected using RT-PCR with human FcRn-specific primers (Fig. 1).

We next carried out a comparative analysis of the uptake and intracellular localization of hIgG1 (HuLys10) (23) and a mutated IgG derived from hIgG1 (His435 to Ala, designated H435A) (13). HuLys10 and the H435A mutant are humanized anti-HEL antibodies. The H435A mutant was used in these studies as it does not bind detectably to mouse or human FcRn (13). SPR was used to exclude the possibility that Alexa 647 labeling might affect the FcRn-binding properties of the IgG (Fig. 2). Immobilized mouse FcRn was used in these analyses as we have found immobilization of human FcRn to the sensor chip results in significant loss of activity (data not shown). Importantly, the binding properties of human and mouse FcRn to hIgG1 and H435A are similar (13), validating the use of mouse FcRn. The SPR analyses showed that the labeled hIgG1 bound to FcRn in a pH-dependent way [binding at pH 6.0 with rapid dissociation at pH 7.2, as shown for unlabeled Fc fragments or IgG in earlier studies (25,30)]. In contrast, the labeled H435A mutant did not bind detectably to FcRn at pH 6.0 (Fig. 2) and this was also seen at higher concentrations of H435A (data not shown).

Endothelial cells were pulsed with Alexa 647-labeled IgG (hIgG1 or H435A) in the presence of DiI-LDL. When used in pulse–chase experiments, LDL is a marker for the lysosomal

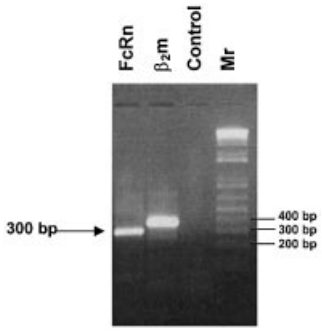

Fig. 1. RT-PCR analysis of FcRn expression in the human endothelial cell line, HULEC-5A. Primers used annealed to bases 799–819 and 1072–1098 of human FcRn, and give the expected product size of 300 bp (12). As a positive control, RT-PCR analysis of β_2-microglobulin was also carried out and gave the predicted product size of 357 bp. Other FcRn-specific primers (see Methods) resulted in products of the predicted sizes (data not shown). 'Control' had no cDNA added to the PCR.

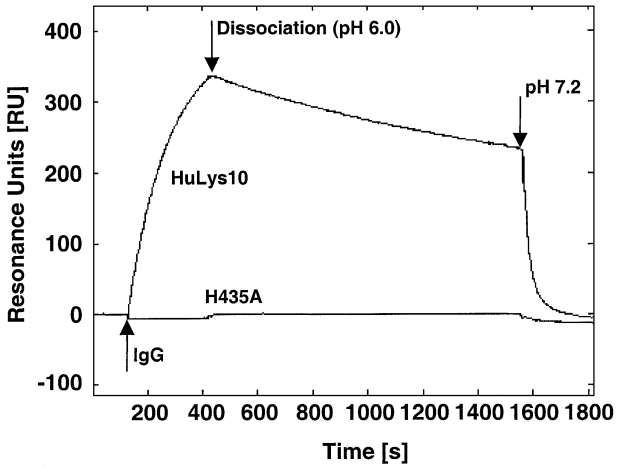

Fig. 2. Analysis of binding of Alexa 647-labeled hIgG1 (HuLys10) and H435A to FcRn. Aliquots of labeling mixes were diluted 10-fold in PBS 6.0 plus 0.01% Tween 20 and injected over a sensor chip coupled with recombinant FcRn. The concentration of IgG injected was 25 μg/ml. The start of the dissociation phase (in PBS 6.0 plus 0.01% Tween 20) is indicated and the effect of injecting PBS 7.2 plus 0.01% Tween 20 is shown.

pathway (26,27). In endothelial cells a scavenger pathway is also involved in LDL uptake, but the scavenger receptor binds only to acetylated LDL (28,29). Following a 20-min pulse of HULEC-5A cells with 5 μg/ml DiI-LDL and 0.25 mg/ml IgG (Alexa 647-labeled wild-type hIgG1 or H435A), the cells were washed and chased in medium containing unlabeled IgG for varying times (0–40 min; Fig. 3). All pulse–chase experiments were carried out at 37°C in medium (depleted of serum IgG) at pH 7. Pulsing at this pH precluded the possibility that IgG binds to cell-surface FcRn prior to uptake, as the FcRn–IgG interaction is not permissive at near neutral pH (25,30). Thus, under the conditions of the experiments IgG uptake occurs via fluid-phase pinocytosis and not via a receptor-mediated process. Following pinocytosis, acidification of endosomal vesicles results in a pH (5.5–6.5) that is permissive for the FcRn–IgG interaction (25, 30).

Figure 3 shows that there are marked differences between the trafficking of wild-type hIgG1 and the H435A mutant. For all chase times, there is significantly more H435A than wild-type hIgG1 within the cells and this cannot be accounted for by different labeling efficiencies of the IgG (see Methods). H435A shows extensive co-localization with the lysosomal pathway marker, LDL, at all chase times. When it can be detected, wild-type hIgG1 is also co-localized with LDL, although the low intensity of the hIgG1 signal makes this difficult to visualize. Similar results were obtained for both the recombinant antibody, HuLys10, and commercially available polyclonal hIgG1 (Fig. 3), indicating that these observations are not restricted to HuLys10. The use of the lysosomal tracer dextran (M_r 10,000) also resulted in significant co-localization with H435A (Fig. 3). In contrast to LDL, dextran is taken up via a fluid-phase rather than via a receptor-mediated process. As an additional control in these experiments, HULEC-5A cells were pulse-chased with Alexa 488-labeled Tf. With no chase, Tf uptake could be seen as punctate vesicles throughout the cytoplasm (data not shown). As expected from earlier studies in different cell types (26), Tf was nearly undetectable after a 10-min chase and had disappeared to below detectable levels following a 20-min chase (data not shown).

In earlier studies, we have shown that wild-type mIgG1 does not bind detectably to human FcRn (16). We therefore analyzed the uptake and trafficking of Alexa 647-labeled mIgG1, using similar methods to those described above. The labeling efficiencies of mIgG1 and hIgG1 used in these analyses were very similar (see Methods). mIgG1 behaves in a way that is indistinguishable from H435A, with a substantial amount of co-localization with LDL at both early and late chase times (Fig.4). The lysosomal fate of mIgG1 gives an explanation at the cellular level as to why mIgG1 is cleared rapidly from the circulation in humans (31,32).

We next analyzed the uptake of IgG using concentrations that were closer to physiological levels [11–12 mg/ml (33)]. hIgG1 or mIgG1 were added at concentrations ranging from 0.25 to 2.5 mg/ml in the presence of DiI-LDL. Due to technical limitations, the amount of added IgG was not increased >2.5 mg/ml. Following a 20-min pulse, the distribution of IgG was analyzed following a 20-min chase for concentrations ranging from 0.25 to 2.5 mg/ml IgG. For all concentrations of mIgG1, extensive co-localization with LDL was seen (Fig. 5A). At higher concentrations of mIgG1, greater accumulation of mIgG1 was consistently seen relative to that at lower concentrations (Fig. 5). Variation of the concentration of hIgG1 had marked effects on accumulation and co-localization with LDL (Fig. 5A): at low concentrations, and consistent with the data shown in Figs 3 and 4, limited uptake was seen which was difficult to detect in most cells. However, an increase in both hIgG1 accumulation and trafficking to lysosomes was seen as the concentration was increased from 0.25 to 2.5 mg/ml. Similar results were seen for 40-min chase times (data not shown). Flow cytometric analyses were used to quantitate the uptake of fluorescently labeled IgG (Fig. 5B). For both mIgG1 and hIgG1, uptake increased as more IgG was added during the pulsing of the cells. At all concentrations of IgG, mIgG1 accumulated to 2- to 3-fold greater levels in the cells relative to hIgG1 (Fig. 5B). Again, this difference could not be explained

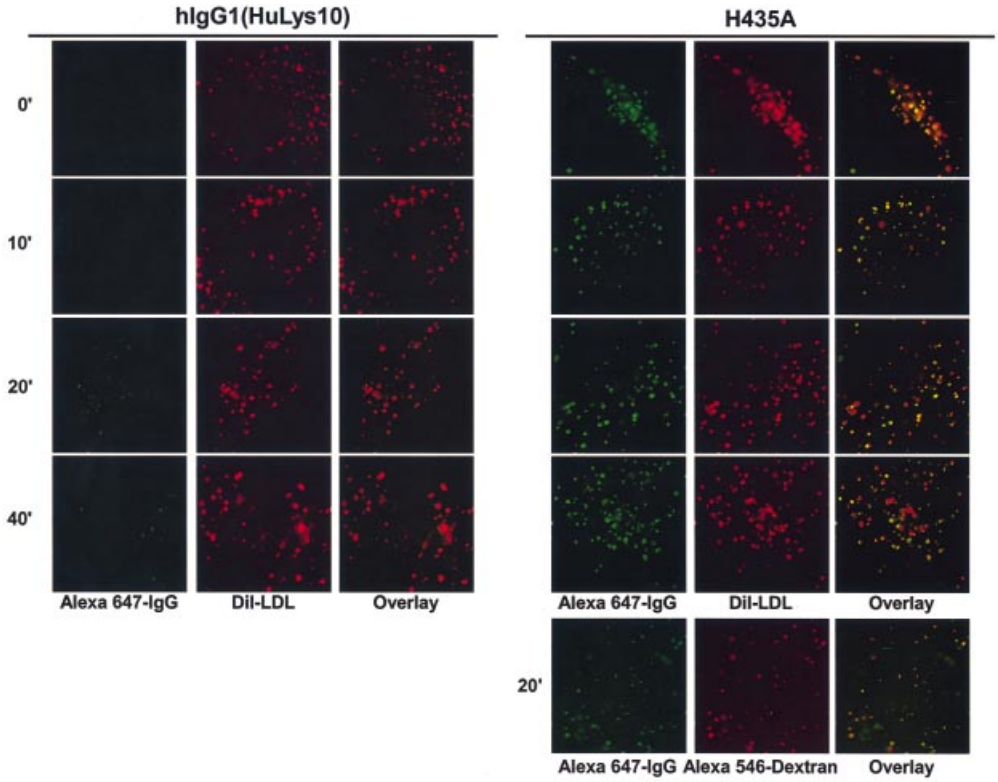

Fig. 3. Fate of Alexa 647-labeled wild-type hIgG1 (HuLys10) or mutated variant (H435A) in HULEC-5A cells. Cells were pulsed with 0.25 mg/ml IgG and 5 μg/ml DiI-LDL, and chased for 0, 10, 20 and 40 min. The lower right-hand panel shows data for cells that were pulsed with 0.25 mg/ml H435A and 0.5 mg/ml Alexa 546-labeled dextran, and chased for 20 min. Images were acquired and processed as described in Methods. Representative cells from at least five independent experiments for DiI-LDL/IgG treatment and two for dextran/IgG treatment are shown.

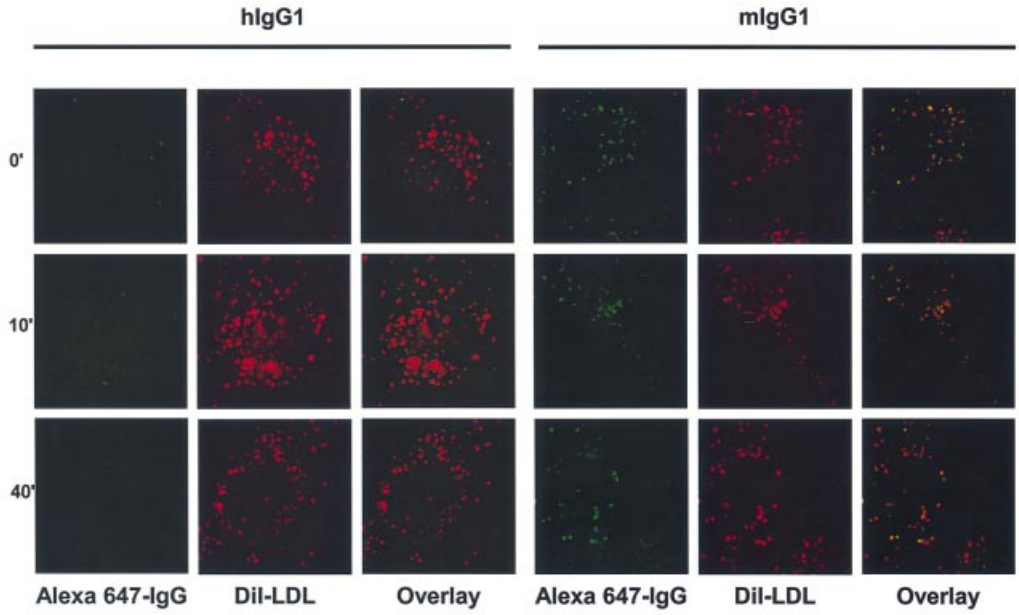

Fig. 4. Fate of Alexa 647-labeled wild-type hIgG1 or mIgG1 in HULEC-5A cells. Cells were pulsed with 0.25 mg/ml IgG and 5 μg/ml DiI-LDL, and chased for 0, 10 and 40 min. Images were acquired and processed as described in Methods. Data show representative cells from at least four independent experiments.

by lower labeling efficiency of hIgG1 relative to mIgG1 as in the experiment shown, Alexa 647 incorporation into hIgG1 was slightly greater than that for mIgG1.

We further investigated the trafficking of IgG by immunofluorescence staining with anti-EEA1, an early endosomal marker. HULEC-5A cells which had been pulsed with Alexa 647-labeled H435A and then chased for 0 or 20 min were stained with this marker. These analyses demonstrated that following uptake, IgG is primarily seen in early endosomes (Fig. 6). Subsequently, the IgG trafficks into EEA1-negative vesicles (Fig. 6). H435A therefore migrates through early endosomes en route to lysosomes and similar results were observed for wild-type hIgG1 (data not shown).

Discussion

In the current study we have used fluorescence imaging to investigate the fate of IgG following pinocytic uptake into human endothelial cells. Microvasculature-derived endothelial cells are believed to be a major site of serum IgG homeostasis (9). We have compared hIgG1 and a variant in which mutation of a key contact residue for FcRn binding (13,14,20) results in loss of detectable interaction with FcRn. Our observations provide experimental support for the hypothesis which was originally proposed by Brambell *et al*. (1), and expounded upon later in more detail (10,11), to explain the mechanism at the (intra)cellular level by which serum IgG homeostasis is maintained: IgG molecules are taken up by endothelial cells and if they bind to FcRn, are recycled or transcytosed. In contrast, IgG molecules that do not bind to FcRn enter the cells and are trafficked into the lysosomal route where they undergo degradation. Our analyses also indicate that FcRn is saturable and provide some insight into the capacity of the homeostatic system.

Our studies demonstrate that IgG (mutated hIgG1 or mIgG1) that do not bind to human FcRn accumulate in endothelial cells and enter the lysosomal pathway. In contrast, at relatively low concentrations (0.25 mg/ml), IgG such as wild-type hIgG1 which bind to FcRn accumulate in cells at significantly lower levels. By fluorescence microscopy, these levels are almost indistinguishable from background levels. Trivial reasons for this difference in behavior between the IgG, such as different labeling efficiencies, source of hIgG1, etc., have been excluded. Thus, at steady state the recycling (or transcytotic) compartment for FcRn–IgG complexes appears to be difficult to detect at relatively low concentrations of IgG. This suggests that recycling is very rapid or involves limited numbers of vesicles/receptors or both. Others have reported that recycling vesicles containing fluorescently labeled Tf may result in more diffuse staining (26). The possibility that the difficulty in detecting hIgG1 (HuLys10 or commercially available hIgG1) inside cells when used at 0.25 mg/ml is due to inefficient uptake is made unlikely by the observation that under the same conditions, the mutant H435A or mIgG1 accumulate to significant, readily detectable levels in the cells. Since the only difference between wild-type hIgG1 and the H435A mutant is a single amino acid change that affects FcRn binding, we would not expect efficiencies of uptake to differ. This mutation is known to have no effect on binding to FcγRI, II and III or C1q (13), indicating that it does not cause perturbations in the conformation of the Fc region. Further, if the mutation affected binding to an as yet unknown surface receptor that might be involved in uptake and delivery of IgG to FcRn in acidic, intracellular compartments [permissive for FcRn binding (25,30)], then it is unlikely that the H435A mutation would serendipitously enhance binding. Similar arguments would be expected to hold for the less closely related mIgG1. Thus, uptake of both wild-type hIgG1 and H435A/mIgG1 is apparently efficient, but the retention of the two classes of ligands shows marked differences.

When the concentration of wild-type hIgG1 is increased to higher levels (0.5–2.5 mg/ml), significant co-localization with the lysosomal pathway marker, LDL, is seen. Quantitative analyses using flow cytometry indicate that as the concentration of hIgG1 is increased, the accumulation of labeled IgG in the cells increases. A similar effect of concentration increase is seen for mIgG1. However, for a given IgG concentration, the levels of mIgG1 that accumulate in the cells are consistently 2- to 3-fold higher than those of hIgG1. As a consequence, co-localization of mIgG1 with LDL can be clearly seen at even the lowest concentration (0.25 mg/ml) of mIgG1 used. The observations for wild-type hIgG1 demonstrate that FcRn is saturable in its role as a salvage receptor, which is a prerequisite if it is to act as a homeostat. Perhaps unexpectedly, however, trafficking of hIgG1 into the lysosomal pathway can be readily detected at a concentration of exogenous IgG of 0.5 mg/ml (~3 μM), which is significantly lower than the levels of circulating IgG in humans [11–12 mg/ml (33)]. It is probable that lysosomal trafficking occurs at even lower concentrations of hIgG1, but is undetectable due to the limitations of fluorescence microscopy. This trafficking into the lysosomal route, which presumably precedes degradation, is consistent with earlier biochemical studies in *ex vivo* human placental models showing that during IgG transcytosis a significant proportion of IgG is degraded (13,34). Similarly, high levels of degradation occur during the transport of IgG across the rodent yolk sac (35) and neonatal intestine (36). However, and in contrast to the current analyses, the precise levels of endogenous IgG were not known in these studies of IgG transport (13,34–36). FcRn has evolved to carry out diverse roles involving both IgG transport and homeostasis (10,11). As a consequence of using a 'shared' receptor, IgG degradation therefore appears to be an undesirable side-reaction that occurs during processes such as delivery of maternal IgG, for which transcytosis without any degradation would be optimal.

Our earlier analyses showed that mIgG1 does not bind detectably to soluble, recombinant human FcRn (16), which provided a possible reason for the short serum half-life of mIgG1 in humans (31,32). Here, we demonstrate that in human endothelial cells, mIgG1 is efficiently taken up from the extracellular medium into the lysosomal pathway where it most likely undergoes degradation. Lysosomal trafficking appears to be relatively independent of the concentration of exogenous mIgG1 added. These studies therefore provide an explanation at the cellular level for the rapid catabolic rates of mIgG1 in humans (31,32) and this has implications for the effective use of such antibodies in therapy.

Although earlier studies have analyzed the trafficking of IgG in FcRn-transfected epithelial cells (37–39) and untransfected

placental endothelial (40) or trophoblast cells (41), in these analyses the intracellular fate of IgG ligands which do not bind to FcRn was not analyzed. In several analyses, prebinding of IgG to cell surface FcRn at pH 6.0 had to be carried out for significant uptake of IgG to be seen (37–39) and this is most likely due to the lower concentrations of IgG used. By analyzing the concentration dependence of IgG passage into the lysosomal pathway, we have obtained clear evidence

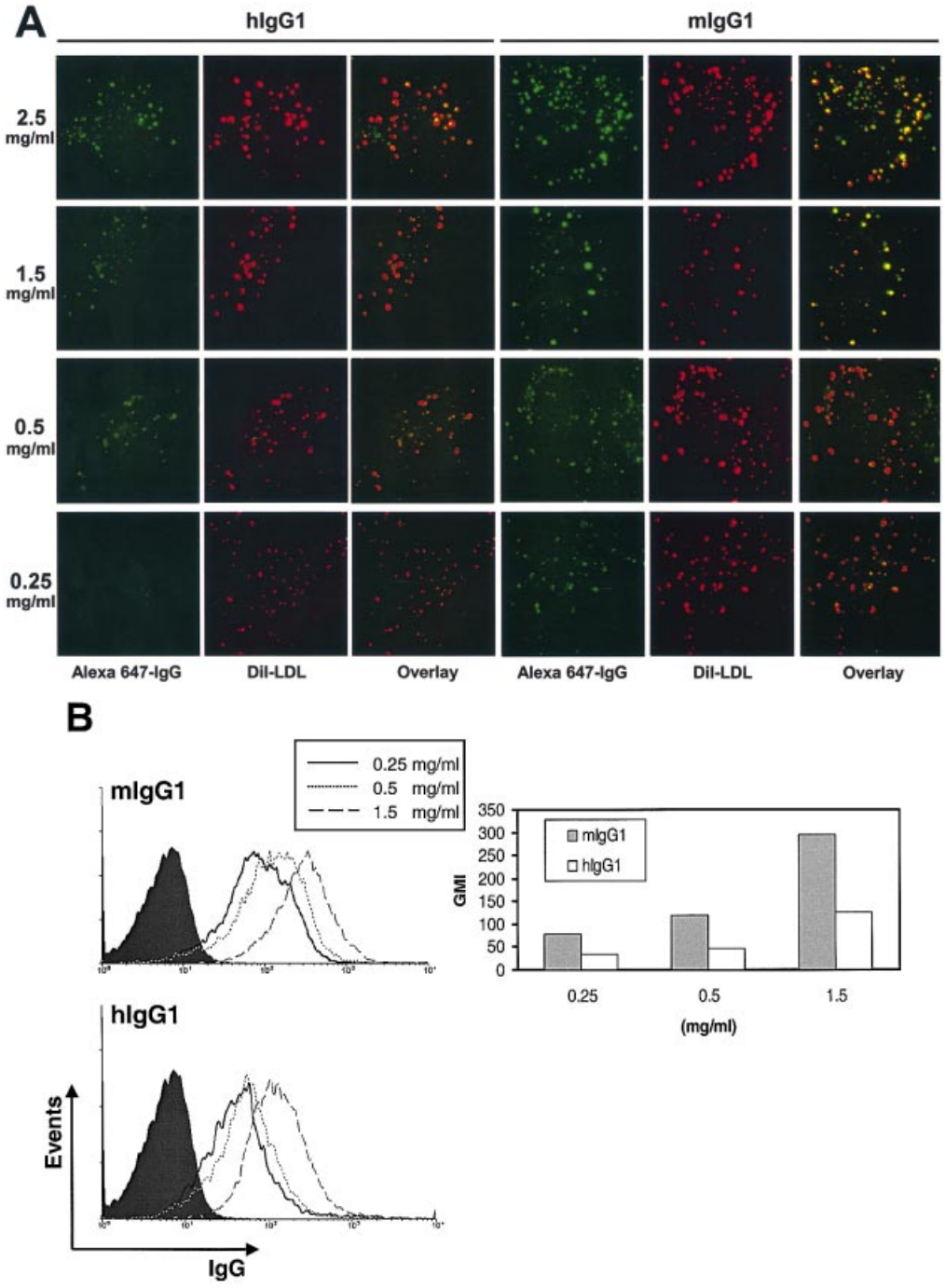

Fig. 5. (A) Concentration dependence of IgG uptake by HULEC-5A cells. Cells were pulsed for 20 min with the concentrations shown of Alexa 647-labeled wild-type hIgG1 or mIgG1 and 5 μg/ml DiI-LDL, and then chased for 20 min. Images were acquired and processed as described in Methods. Data show representative cells from two independent experiments. (B) Flow cytometric analysis of uptake of Alexa 647-labeled IgG by HULEC-5A cells pulsed with different concentrations (0.25–1.5 mg/ml) of wild-type hIgG1 or mIgG1 and chased for 20 min. Filled histograms represent cells treated with medium only. GMI = geometric mean intensity following subtraction of autofluorescence levels (5.9). Data are representative of two experiments,

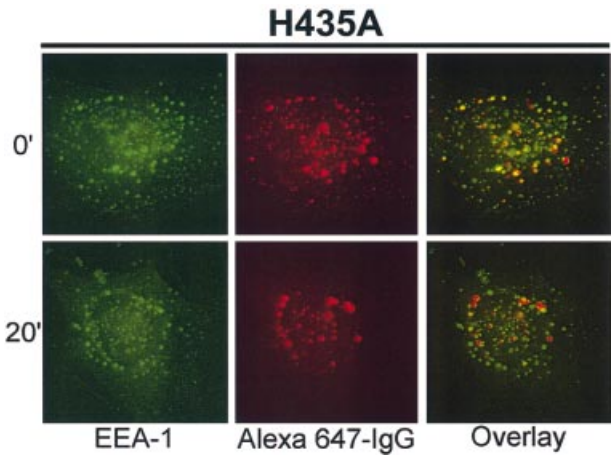

Fig. 6. Analysis of trafficking of H435A into early endosomes. Cells were pulsed for 20 min with 1 mg/ml Alexa 647-labeled H435A and chased for 0 or 20 min. Cells were fixed, permeabilized and stained with anti-EEA1 followed by Alexa 488-labeled anti-mIgG. Images were acquired and processed as described in Methods. Data show representative cells from two independent experiments.

for saturability of FcRn in microvasculature-derived endothelial cells that express this Fc receptor at physiological levels. In this context, higher levels of FcRn expression in transfected cells, lower concentrations of exogenous IgG and/or lack of expression of human β_2-microglobulin (39) might account for the apparent differences in lysosomal trafficking of IgG in our study and that of Praetor *et al.* (37).

It is possible that our observations concerning human FcRn and its ligands can be extrapolated to other species. However, although it was previously believed that data in mice could be extended to humans (42–44), this has recently been shown to not always be the case (16). Unexpectedly, human and mouse FcRn have been found to show marked differences in binding specificity for IgG from different species, with human FcRn being highly selective relative to the highly promiscuous mouse FcRn (16). Thus, although mouse and human FcRn share a high degree of homology (12,45), there may be other differences in the behavior of human and mouse FcRn which could impinge on the intracellular routing, IgG capacity, etc. Indeed, the different ratios of vascular area:-blood volume and different circulating levels of IgG might be expected to necessitate variations in FcRn properties across species.

In summary, our data provide support for a role for FcRn in salvaging IgG from degradation in human endothelial cells. The analysis of trafficking of two closely related antibodies which differ only in their affinity for FcRn has allowed us to infer that the alterations in IgG trafficking that we observe are due to differences in handling by FcRn. Thus, these studies impact on the molecular and cellular mechanisms involved in IgG homeostasis. Our observations are of significance for the understanding and treatment of disorders involving abnormalities in IgG levels. They also have relevance to the effective application of therapeutic antibodies, where serum persistence is known to be a critical parameter.

Acknowledgements

Cruz Martinez, Carlos Vaccaro and Palmer Long provided valuable assistance with the fluorescence microscopy. We are indebted to Steve Duffy for advice concerning maintenance of HULEC-5A cells and to Francisco Candal (Centers for Disease Control) for providing the cells. These studies were supported by grants R01 AI 39167 (E. S. W.) and R01 AI/RR 50747 (R. J. O.) from the National Institutes of Health.

Abbreviations

FcRn	neonatal Fc receptor
HEL	hen egg lysozyme
hIgG	human IgG
IVIg	i.v. Ig
LDL	low-density lipoprotein
mIgG	mouse IgG
SPR	surface plasmon resonance
Tf	transferrin

References

1 Brambell, F. W. R., Hemmings, W. A. and Morris, I. G. 1964. A theoretical model of γ-globulin catabolism. *Nature* 203:1352.
2 Ghetie, V., Hubbard, J. G., Kim, J. K., Tsen, M. F., Lee, Y. and Ward, E. S. 1996. Abnormally short serum half-lives of IgG in beta 2-microglobulin-deficient mice. *Eur. J. Immunol.* 26:690.
3 Junghans, R. P. and Anderson, C. L. 1996. The protection receptor for IgG catabolism is the beta2-microglobulin-containing neonatal intestinal transport receptor. *Proc. Natl Acad. Sci. USA* 93:5512.
4 Israel, E. J., Wilsker, D. F., Hayes, K. C., Schoenfeld, D. and Simister, N. E. 1996. Increased clearance of IgG in mice that lack beta 2-microglobulin: possible protective role of FcRn. *Immunology* 89:573.
5 Rodewald, R. and Kraehenbuhl, J. P. 1984. Receptor-mediated transport of IgG. *J. Cell Biol.* 99:159s.
6 Simister, N. E. and Rees, A. R. 1985. Isolation and characterization of an Fc receptor from neonatal rat small intestine. *Eur. J. Immunol.* 15:733.
7 Zijlstra, M., Bix, M., Simister, N. E., Loring, J. M., Raulet, D. H. and Jaenisch, R. 1990. Beta 2-microglobulin deficient mice lack $CD4^-8^+$ cytolytic T cells. *Nature* 344:742.
8 Israel, E. J., Patel, V. K., Taylor, S. F., Marshak-Rothstein, A. and Simister, N. E. 1995. Requirement for a beta 2-microglobulin-associated Fc receptor for acquisition of maternal IgG by fetal and neonatal mice. *J. Immunol.* 154:6246.
9 Borvak, J., Richardson, J., Medesan, C., Antohe, F., Radu, C., Simionescu, M., Ghetie, V. and Ward, E. S. 1998. Functional expression of the MHC class I-related receptor, FcRn, in endothelial cells of mice. *Int. Immunol.* 10:1289.
10 Ghetie, V. and Ward, E. S. 1997. FcRn: the MHC Class I-related receptor that is more than an IgG transporter. *Int. Immunol.* 18:592.
11 Ghetie, V. and Ward, E. S. 2000. Multiple roles for the major histocompatibility complex class I-related receptor FcRn. *Annu. Rev. Immunol.* 18:739.
12 Story, C. M., Mikulska, J. E. and Simister, N. E. 1994. A major histocompatibility complex class I-like Fc receptor cloned from human placenta: possible role in transfer of immunoglobulin G from mother to fetus. *J. Exp. Med.* 180:2377.
13 Firan, M., Bawdon, R., Radu, C., Ober, R. J., Eaken, D., Antohe, F., Ghetie, V. and Ward, E. S. 2001. The MHC class I related receptor, FcRn, plays an essential role in the maternofetal transfer of gammaglobulin in humans. *Int. Immunol.* 13:993.
14 Medesan, C., Matesoi, D., Radu, C., Ghetie, V. and Ward, E. S. 1997. Delineation of the amino acid residues involved in transcytosis and catabolism of mouse IgG1. *J. Immunol.* 158:2211.
15 Ghetie, V., Popov, S., Borvak, J., Radu, C., Matesoi, D., Medesan, C., Ober, R. J. and Ward, E. S. 1997. Increasing the serum

persistence of an IgG fragment by random mutagenesis. *Nat. Biotechnol.* 15:637.
16 Ober, R. J., Radu, C. G., Ghetie, V. and Ward, E. S. 2001. Differences in promiscuity for antibody–FcRn interactions across species: implications for therapeutic antibodies. *Int. Immunol.* 13:1551.
17 Burmeister, W. P., Huber, A. H. and Bjorkman, P. J. 1994. Crystal structure of the complex of rat neonatal Fc receptor with Fc. *Nature* 372:379.
18 Kim, J. K., Tsen, M. F., Ghetie, V. and Ward, E. S. 1994. Localization of the site of the murine IgG1 molecule that is involved in binding to the murine intestinal Fc receptor. *Eur. J. Immunol.* 24:2429.
19 Medesan, C., Radu, C., Kim, J. K., Ghetie, V. and Ward, E. S. 1996. Localization of the site of the IgG molecule that regulates maternofetal transmission in mice. *Eur. J. Immunol.* 26:2533.
20 Martin, W. L., West, A. P. J., Gan, L. and Bjorkman, P. J. 2001. Crystal structure at 2.8 Å of an FcRn/heterodimeric Fc complex: mechanism of pH dependent binding. *Mol. Cell* 7:867.
21 Shields, R. L., Namenuk, A. K., Hong, K., Meng, Y. G., Rae, J., Briggs, J., Xie, D., Lai, J., Stadlen, A., Li, B., Fox, J. A. and Presta, L. G. 2001. High resolution mapping of the binding site on human IgG1 for Fc gamma RI, Fc gamma RII, Fc gamma RIII, and FcRn and design of IgG1 variants with improved binding to the Fc gamma R. *J. Biol. Chem.* 276:6591.
22 Raghavan, M., Chen, M. Y., Gastinel L. N. and Bjorkman, P. J. 1994. Investigation of the interaction between the class I MHC-related Fc receptor and its immunoglobulin G ligand. *Immunity* 1:303.
23 Foote, J. and Winter, G. 1992. Antibody framework residues affecting the conformation of the hypervariable loops. *J. Mol. Biol.* 224:487.
24 Ghetie, M. A., Tucker, K., Richardson, J., Uhr J. W. and Vitetta, E. S. 1992. The anti-tumor activity of an anti-CD22 immunotoxin in SCID mice with disseminated Daudi lymphoma is enhanced by either an anti-CD19 antibody or an anti-CD19 immunotoxin. *Blood* 80:2315.
25 Popov, S., Hubbard, J. G., Kim, J., Ober, B., Ghetie, V. and Ward, E. S. 1996. The stoichiometry and affinity of the interaction of murine Fc fragments with the MHC class I-related receptor, FcRn. *Mol. Immunol.* 33:521.
26 Ghosh, R. N., Gelman, D. L. and Maxfield, F. R. 1994. Quantification of low density lipoprotein and transferrin endocytic sorting HEp2 cells using confocal microscopy. *J. Cell Sci.* 107:2177.
27 Mayor, S., Presley, J. F. and Maxfield, F. R. 1993. Sorting of membrane components from endosomes and subsequent recycling to the cell surface occurs by a bulk flow process. *J. Cell Biol.* 121:1257.
28 Brown, M. S., Goldstein, J. L., Krieger, M., Ho, Y. K. and Anderson, R. G. 1979. Reversible accumulation of cholesteryl esters in macrophages incubated with acetylated lipoproteins. *J. Cell Biol.* 82:597.
29 Brown, M. S., Basu, S. K., Falck, J. R., Ho, Y. K. and Goldstein, J. L. 1980. The scavenger cell pathway for lipoprotein degradation: specificity of the binding site that mediates the uptake of negatively-charged LDL by macrophages. *J. Supramol. Struct.* 13:67.
30 Raghavan, M., Bonagura, V. R., Morrison, S. L. and Bjorkman, P. J. 1995. Analysis of the pH dependence of the neonatal Fc receptor/immunoglobulin G interaction using antibody and receptor variants. *Biochemistry* 34:14649.
31 Saleh, M. N., Khazaeli, M. B., Wheeler, R. H., Dropcho, E., Liu, T., Urist, M., Miller, D. M., Lawson, S., Dixon, P. and Russell, C. H. 1992. Phase I trial of the murine monoclonal anti-GD2 antibody 14G2a in metastatic melanoma. *Cancer Res.* 52:4342.
32 Frodin, J. E., Lefvert, A. K. and Mellstedt, H. 1990. Pharmacokinetics of the mouse monoclonal antibody 17-1A in cancer patients receiving various treatment schedules. *Cancer Res.* 50:4866.
33 Waldmann, T. A. and Strober, W. 1969 Metabolism of immunoglobulins. *Prog. Allergy* 13:1.
34 Contractor, S. F., Eaton, B. M. and Stannard, P. J. 1983. Uptake and fate of exogenous immunoglobulin G in the perfused human placenta. *J. Reprod. Immunol.* 5:265.
35 Wild, A. E. 1981. Endocytic mechanism in protein transfer across the placenta. *Placenta Suppl.* 1:165.
36 Rodewald, R. B. 1976. Intestinal transport of peroxidase-conjugated IgG fragments in the neonatal rat. In Hemmings, W. A., ed., *Maternofetal Transmission of Immunoglobulins*, p. 137. Cambridge University Press, Cambridge.
37 Praetor, A., Ellinger, I. and Hunziker, W. 1999. Intracellular traffic of the MHC class I-like IgG Fc receptor, FcRn, expressed in epithelial MDCK cells. *J. Cell Sci.* 112:2291.
38 McCarthy, K. M., Yoong, Y. and Simister, N. E. 2000. Bidirectional transcytosis of IgG by the rat neonatal Fc receptor expressed in a rat kidney cell line: a system to study protein transport across epithelia. *J. Cell Sci.* 113:1277.
39 Claypool, S. M., Dickinson, B. L., Yoshida, M., Lancer, W. I. and Blumberg, R. S. 2002. Functional reconstitution of human FcRn in Madin-Darby canine kidney cells requires co-expressed human β_2-microglobulin. *J. Biol. Chem.* 277:28038.
40 Antohe, F., Radulescu, L., Gafencu, A., Ghetie, V. and Simionescu, M. 2001. Expression of functionally active FcRn and the differentiated bidirectional transport of IgG in human placental endothelial cells. *Hum. Immunol.* 62:93.
41 Ellinger, I., Schwab, M., Stefanescu, A., Hunziker, W. and Fuchs, R. 1999. IgG transport across trophoblast-derived BeWo cells: a model system to study IgG transport in the placenta. *Eur. J. Immunol.* 29:733.
42 Bazin, R., Boucher, G., Monier, G., Chevrier, M. C., Verrette, S., Broly, H. and Lemieux, R. 1994. Use of hu-IgG-SCID mice to evaluate the *in vivo* stability of human monoclonal IgG antibodies. *J. Immunol. Methods* 172:209.
43 Zuckier, L. S., Georgescu, L., Chang, C. J., Scharff, M. D. and Morrison, S. L. 1994. The use of severe combined immunodeficiency mice to study the metabolism of human immunoglobulin G. *Cancer* 73:794.
44 Kim, J. K., Firan, M., Radu, C. G., Kim, C. H., Ghetie, V. and Ward, E. S. 1999. Mapping the site on human IgG for binding of the MHC class I-related receptor, FcRn. *Eur. J. Immunol.* 29:2819.
45 Ahouse, J. J., Hagerman, C. L., Mittal, P., Gilbert, D. J., Copeland, N. G., Jenkins, N. A. and Simister, N. E. 1993. Mouse MHC class I-like Fc receptor encoded outside the MHC. *J. Immunol.* 151:6076.